

**Crystal structures in generalized Skyrme model**I. Perapechka<sup>1</sup> and Ya. Shnir<sup>1,2,3</sup><sup>1</sup>*Department of Theoretical Physics and Astrophysics, BSU, Minsk 220004, Belarus*<sup>2</sup>*BLTP, JINR, Dubna 141980, Moscow Region, Russia*<sup>3</sup>*Department of Theoretical Physics, Tomsk State Pedagogical University, Tomsk 634041, Russia*

(Received 4 April 2017; published 17 August 2017)

We investigate the properties of triply periodic Skyrme crystals in the generalized Skyrme model  $\mathcal{L}_6 + \mathcal{L}_4 + \mathcal{L}_2 + \mathcal{L}_0$  with higher-derivative terms up to sixth order. Three different symmetry breaking potential terms  $\mathcal{L}_0$  are considered, the generalized pion mass term, double-vacuum potential, and mixed potential. Various scenarios of phase transitions from the low-density phase to the high-density phase are examined for different choices of the parameters of the model. In particular, we investigated limiting behavior of the Skyrme crystals in the truncated submodel without the Skyrme term  $\mathcal{L}_4$  and/or without the  $\mathcal{L}_2$  term. We show that the Skyrme crystal may exist in the pure  $\mathcal{L}_4$  and  $\mathcal{L}_6$  models and investigated the phase structure of these solutions. Considering the near-Bogomolny-Prasad-Sommerfeld submodel, we found that there are indications of the phase transition from a low-density quasi-liquid phase to the high-density symmetric phase of the Skyrmonic matter.

DOI: [10.1103/PhysRevD.96.045013](https://doi.org/10.1103/PhysRevD.96.045013)**I. INTRODUCTION**

In 1961 Skyrme proposed a simple version of the nonlinear sigma model [1], which can be considered as an effective low-energy theory of pions. It was suggested to consider baryons as topological solitons, with identification of the baryon number and the topological charge  $B$  of the field configuration. In this picture, the pions correspond to the linearized fluctuations of the baryon field; the potential term is necessary to give a mass to these fluctuations.

The Skyrme model has received much attention during the last few decades. There is a variety of soliton solutions constructed numerically [2–4]. While the simplest configuration of degree  $B = 1$  is spherically symmetric, the Skyrmions of higher topological degrees possess much more complicated symmetries: they are symmetric with respect to the dihedral group  $D_n$ , the extended dihedral groups  $D_{nh}$  or  $D_{nd}$ , or even the icosahedral group  $I_h$  [4]. Certainly, there is a similarity with symmetries of crystals and fullerenes. Indeed, one can arrange the Skyrmions in a crystalline structure that is periodic in all three space dimensions [5–8].

A feature of the usual Skyrme model is that the soliton solutions do not saturate the topological bound; the binding energy is relatively high. This observation does not agree with experimentally known low binding energies of physical nuclei; the difference is more than an order of magnitude. It was also observed that the energies of the configurations of higher degrees slowly approach the topological bound as  $B$  increases; see, e.g., [9]. Other important observations was that the increase of the pion mass may strongly affect the structure of the multi-Skyrmion configurations [10].

Recently a few modifications of the Skyrme model were proposed to improve its phenomenological predictions and construct weakly bounded multisoliton configurations [14–11]]. Two possible directions there are related with a generalization of the original Skyrme model by inclusion into Lagrangian some additional terms which are higher order in derivatives [11,15–17], or by a nonstandard choice of the potential term, which would decrease the attractive force between the Skyrmions [13,14,18]. In the first case there is a possibility to truncate the model to the so-called Bogomolny-Prasad-Sommerfeld (BPS) submodel [19], which is invariant under volume preserving diffeomorphisms [11,20]. Multisoliton solutions of this reduced model exactly saturate the topological bound; they may interact only elastically and the configuration in some sense resembles the system of liquid drops. In the second case, the repulsive part of the potential separates the constituents of the multi-Skyrmion configuration which resembles a loosely bound collection of almost isolated spherically symmetric unit charge solitons.

In this paper, we will study the Skyrmion crystals in the generalized model with sextic term and with various choices of the potential. In particular, we investigate what happens to the Skyrme crystal as the system deforms away from the standard Skyrme model. The parameters we vary are the coefficients at all terms of the extended model, so both the usual Skyrme model and its self-dual truncation are the limiting cases. As we shall see, there are indications of phase transition from a low-density quasi-liquid phase to the high-density symmetric phase of Skyrmonic matter in the reduced almost self-dual model.

The paper is organized as follows: in the next two sections we discuss the construction and the symmetries of

the generalized Skyrme crystal. The numerical results for the three different symmetry breaking potential terms, which include the generalized pion mass term, double-vacuum potential, and mixed potential, are presented in Sec. IV. Here we also compare the results to the usual pattern of phase transitions in the conventional Skyrme model and describe a numerical scheme we implement to find the energy minimizers. The Skyrme crystals in the submodels of the general model are discussed in Sec. V. We give our conclusions, remarks, and possible future directions of development in the final section.

## II. GENERALIZED SKYRME MODEL

The general Skyrme model is a Poincaré invariant, nonlinear sigma model field theory. The most general allowed form of it, restricted by the condition that the corresponding Hamiltonian must be quadratic in time derivatives, is

$$\mathcal{L}_{0246} = \mathcal{L}_2 + \mathcal{L}_4 + \mathcal{L}_6 + \mathcal{L}_0, \quad (1)$$

where  $\mathcal{L}_0 = m_\pi^2 \mathcal{V}$  is a potential term with parameter  $m_\pi^2$  [21]. The usual structure of the Skyrme model is given by the two terms

$$\mathcal{L}_2 = \frac{a}{2} \text{Tr}(L_\mu L^\mu), \quad \mathcal{L}_4 = \frac{b}{4} \text{Tr}([L_\mu, L_\nu][L^\mu, L^\nu]), \quad (2)$$

where  $a$  and  $b$  are non-negative coupling constants and

$$L_\mu = U^\dagger \partial_\mu U \quad (3)$$

is the  $\mathfrak{su}(2)$ -valued left-invariant current, associated with the  $SU(2)$ -valued scalar field  $U = \sigma \cdot \mathbb{1} + i\boldsymbol{\pi} \cdot \boldsymbol{\tau}$ . It can be represented in terms of the quartet of scalar fields  $\mathbf{n} = (\sigma, \boldsymbol{\pi})$  restricted to the surface of the unit sphere  $S^3$ ,  $\mathbf{n}^2 = \sigma^2 + \boldsymbol{\pi} \cdot \boldsymbol{\pi} = 1$ .

The field of the model is required to satisfy the boundary condition  $U(\mathbf{x}) \rightarrow \mathbb{1}$  as  $\mathbf{x} \rightarrow \infty$ ; thus, the field is a map  $U: S^3 \mapsto S^3$  labeled by the topological invariant  $B = \pi_3(S^3)$ . Explicitly, the winding number of the field configuration is given by

$$\begin{aligned} B &= \frac{1}{24\pi^2} \int d^3x \varepsilon^{ijk} \text{tr}[(U^\dagger \partial_i U)(U^\dagger \partial_j U)(U^\dagger \partial_k U)] \\ &= \frac{1}{24\pi^2} \int d^3x \varepsilon^{ijk} \text{tr}[L_i L_j L_k] \\ &= -\frac{1}{12\pi^2} \int d^3x \varepsilon_{abcd} \varepsilon^{ijk} n^a \partial_i n^b \partial_j n^c \partial_k n^d. \end{aligned} \quad (4)$$

The corresponding topological current is

$$B^\mu = \frac{1}{24\pi^2} \varepsilon^{\mu\nu\rho\sigma} \text{Tr}(L_\nu L_\rho L_\sigma). \quad (5)$$

Thus, the model (1) includes a sextic term

$$\mathcal{L}_6 = 4\pi^4 c B_\mu B^\mu, \quad (6)$$

where  $c$  is another non-negative coupling constant. Note that the usual rescaling of the spatial coordinates  $\mathbf{x} \rightarrow \sqrt{\frac{a}{b}} \mathbf{x}$  allows us to set two of the coupling constants to unity. However, in order to study qualitative properties of the solutions numerically, it will be more convenient to keep all four parameters of the model (1).

The choice of the symmetry breaking potential terms  $\mathcal{L}_0$  is important in our discussion. Since we are interested in the study of limiting transition to the self-dual  $\mathcal{L}_0 + \mathcal{L}_6$  crystal, we considered three related potentials [22], the generalized pion mass potential

$$\mathcal{V} = \left( \text{Tr} \left( \frac{\mathbb{1} - U}{2} \right) \right)^\alpha, \quad (7)$$

the double-vacuum potential

$$\mathcal{V} = \left( \text{Tr} \left( \frac{\mathbb{1} + U}{2} \right) \text{Tr} \left( \frac{\mathbb{1} - U}{2} \right) \right)^\alpha \quad (8)$$

and mixed potential

$$\mathcal{V} = \text{Tr} \left( \frac{\mathbb{1} + U}{2} \right) \left( \text{Tr} \left( \frac{\mathbb{1} - U}{2} \right) \right)^\alpha. \quad (9)$$

Here  $\alpha$  is a positive constant which defines the type of asymptotic decay of the field. As  $\alpha = 1$ , the potential (7) is reduced to the usual pion mass potential; setting  $\alpha = 2$  corresponds to the massless potential considered in [13]. The potential (8) corresponds to the so-called ‘‘new’’ potential in the planar Skyrme model [23]; in the limiting case of the self-dual Skyrme submodel it yields the shell-like solutions [22].

Thus, the stress-energy tensor of the general model (1) is given by

$$\begin{aligned} T_{\mu\nu} &= a \text{Tr} \left( L_\mu L_\nu - \frac{1}{2} \eta_{\mu\nu} L_\rho L^\rho \right) \\ &\quad + b \text{Tr} \left( [L_\mu, L_\rho][L_\nu, L^\rho] - \frac{1}{4} \eta_{\mu\nu} [L_\rho, L_\sigma][L^\rho, L^\sigma] \right) \\ &\quad + 8\pi^4 c \left( B_\mu B_\nu - \frac{1}{2} \eta_{\mu\nu} B_\rho B^\rho \right) - \eta_{\mu\nu} m_\pi^2 \mathcal{V}, \end{aligned} \quad (10)$$

where  $\eta_{\mu\nu} = \text{diag}(-1, 1, 1, 1)$  is the usual Minkowski metric. Then, the static energy functional is defined by

$$\begin{aligned}
E &= \int T_{00} d^3x \\
&= \int \{a \partial_i \mathbf{n} \cdot \partial^i \mathbf{n} + 2b((\partial_i \mathbf{n} \cdot \partial^i \mathbf{n})^2 - (\partial_i \mathbf{n} \cdot \partial_j \mathbf{n})(\partial^j \mathbf{n} \cdot \partial^i \mathbf{n})) \\
&\quad + c(\epsilon^{abcd} \partial_1 n_a \partial_2 n_b \partial_3 n_c n_d)^2 + m_\pi^2 \mathcal{V}\} d^3x. \quad (11)
\end{aligned}$$

The energies of the Skyrmions satisfy the topological bound

$$E \geq E_1 |B|. \quad (12)$$

Setting the parameters of the model as  $a = 1$ ,  $b = 1$ ,  $c = m_\pi = 0$ , we obtain  $E_1 = 24\pi^2$ . However, on the  $\mathbb{R}^3$  space this bound cannot be saturated; the energy of the static unit charge Skyrmion in the usual Skyrme model without both the sextic term and the potential is  $1.23E_1$ . On the other hand, the truncation of the general model (1) to the self-dual submodel with  $a = b = 0$  allows us to attain an equality in a similar topological bound for that system [11,20].

It is convenient to set the energy unit as the mass of the static Skyrmion in the usual Skyrme model without the sextic term and the potential. Thus, it will be convenient for our purposes to normalize the energy by factor  $1/24\pi^2$ .

### III. GENERALIZED SKYRME CRYSTALS

It was noticed that the topological bound (12) can be approximately saturated by the special arrangement of the Skyrmions in an infinite, triple periodic in a space configuration, the Skyrme crystal [5–8]. This configuration, which can be considered as a model of dense nuclear matter, can be constructed by imposing periodic boundary conditions on the Skyrme field in three spatial dimensions and taking into account that the symmetry generators must combine both the spatial and internal rotations of the Skyrmions. Indeed, the field of the single Skyrmion can be approximated by the triplet of orthogonal dipoles and the character of the interaction between the Skyrmions depends on their relative orientation; there are attractive and repulsive channels in the interaction of two solitons.

Let us consider a cubic cell of size  $L$ , where at the point with spatial coordinates  $(x, y, z)$  the Skyrme field is given by the quartet  $(\sigma, \pi_1, \pi_2, \pi_3)$ . The cell is a building block of the cubic lattice with period  $L$  in all directions. The simplest, low-density case of symmetry of Skyrme crystal was considered by Klebanov [5]. This configuration corresponds to the attractive channel of interaction between the six nearest neighbors; twelve second nearest are in orientation of the repulsive channel. This crystal has combined symmetry generated by

- (i) the spatial translation by  $L$  along the  $x$  axis combined with a rotation by  $\pi$  around the twofold axis in isospin:

$$\begin{aligned}
(x, y, z) &\rightarrow (x + L, y, z), \\
(\sigma, \pi_1, \pi_2, \pi_3) &\rightarrow (\sigma, -\pi_1, \pi_2, -\pi_3); \quad (13)
\end{aligned}$$

- (ii) the spatial reflection in coordinate space combined with internal reflection of  $\mathbf{n}$ :

$$\begin{aligned}
(x, y, z) &\rightarrow (-x, y, z), \\
(\sigma, \pi_1, \pi_2, \pi_3) &\rightarrow (\sigma, -\pi_1, \pi_2, \pi_3); \quad (14)
\end{aligned}$$

- (iii) simultaneous spatial and isospin rotations around a threefold axis:

$$\begin{aligned}
(x, y, z) &\rightarrow (z, x, y), \\
(\sigma, \pi_1, \pi_2, \pi_3) &\rightarrow (\sigma, \pi_3, \pi_1, \pi_2). \quad (15)
\end{aligned}$$

However, such a simple cubic crystal is not a lowest energy configuration for a given value of the lattice period  $L$ . A more detailed analysis reveals that in the usual Skyrme model without the sextic term  $\mathcal{L}_6$ , there are three different phases of the Skyrme crystal with different symmetries.

The body-centered cubic (bcc) lattice of half-Skyrmions [6] corresponds to the higher density. This crystal has symmetries (13), (14), and (15), as well as additional symmetry with respect to a rotation by  $\pi$  around an axis going through the points  $(0, \frac{L}{4}, \frac{L}{2})$  and  $(\frac{L}{2}, \frac{L}{4}, 0)$  in coordinate space, and an O(4) chiral rotation of the field  $\mathbf{n}$ :

$$\begin{aligned}
(x, y, z) &\rightarrow \left(\frac{L}{2} - z, \frac{L}{2} - y, \frac{L}{2} - x\right), \\
(\sigma, \pi_1, \pi_2, \pi_3) &\rightarrow (-\sigma, \pi_2, \pi_1, \pi_3). \quad (16)
\end{aligned}$$

The face-centered cubic (fcc) lattice of Skyrmions [7,8] corresponds to the lower density phase. Here the Skyrmions are placed on the vertices of a cube and more Skyrmions are placed on the center of the faces. There are twelve nearest neighbors in the attractive channel in such a configuration. Its symmetry transformations include both the transformations (14), (15), and a rotation around a fourfold axis in space, combined with the internal SO(3) rotation of the pion field:

$$\begin{aligned}
(x, y, z) &\rightarrow (x, z, -y), \quad (\sigma, \pi_1, \pi_2, \pi_3) \rightarrow (\sigma, \pi_1, \pi_3, -\pi_2) \\
&\quad (17)
\end{aligned}$$

as well as a translation from the corner of a cube to the center of a face combined with an SO(3), isospin rotation acting on  $\boldsymbol{\pi}$ :

$$\begin{aligned}
(x, y, z) &\rightarrow (x + L, y + L, z), \\
(\sigma, \pi_1, \pi_2, \pi_3) &\rightarrow (\sigma, -\pi_1, -\pi_2, \pi_3). \quad (18)
\end{aligned}$$

However, the global minimum of energy of the Skyrme crystal corresponds to the medium-density simple cubic (sc) lattice of half-Skyrmions [8]. This phase is characterized by a spatial translation combined with an SO(4) chiral rotation by  $\pi$  in the  $\sigma, \pi_1$  plane:

$$\begin{aligned} (x, y, z) &\rightarrow (x + L, y, z), \\ (\sigma, \pi_1, \pi_2, \pi_3) &\rightarrow (-\sigma, -\pi_1, \pi_2, \pi_3), \end{aligned} \quad (19)$$

which replaces the transformation (18); however the transformations (14), (15) and (17) are also symmetries of this phase. The minimal energy of the usual Skyrme crystal in the  $\mathcal{L}_2 + \mathcal{L}_4$  model is of  $E = 1.036$  at  $L = 4.71$  in the rescaled units of energy and length.

Note that since the symmetry group of the low-density phase is a subgroup of the symmetry group of a medium-density phase, the phase transition between the fcc and medium density sc phases should be of the second order. Similarly, the transition between the Klebanov sc low-density phase of single Skyrmions and the bcc high-density phase is of second order while the transition from the low-density sc or fcc phases to the bcc lattice is of the first order.

In order to understand the situation better, let us consider a single Skyrmion placed at  $(0, 0, 0)$ , where  $\pi_i = 0$  and  $\sigma = -1$ . The restriction of the reflection symmetry (14) together with the translational invariance (13) means that  $\sigma = 0$  on any surface  $(\pm L, \pm L, \pm L)$ . A cube of side length  $L$  bounded by these surfaces contains a half-Skyrmion with  $\sigma < 0$ . The symmetry restriction (19) also means that  $\sigma = 1$  at the point  $(L, 0, 0)$  where the second half-Skyrmion with  $\sigma > 0$  is located. Each of the cubes has topological charge  $1/2$ . The Skyrme crystal in the high-density phase can be viewed as a construction built from these cubes of two types with Skyrmions appropriately internally rotated; thus, this is a system of half-Skyrmions arranged on a simple cubic lattice.

Our goal now is to study the pattern of phase transition in the general Skyrme crystal (1). Note that direct minimization of the corresponding energy functional needs a large amount of computational power; thus, to simulate the crystal numerically, we follow the approach of Ref. [8]. We expand the unnormalized Skyrme field  $\bar{\mathbf{n}}$  in a Fourier series possessing required symmetries and then minimize the energy with respect to the coefficients of the expansion. The normalized Skyrme field then can be recovered as

$$\mathbf{n} = \frac{\bar{\mathbf{n}}}{\|\bar{\mathbf{n}}\|}.$$

Since the general Skyrme model (1) may have different symmetries, we will look for solutions possessing only general symmetries of the crystal (13)–(15). For such configurations the Fourier expansion will take the form

$$\begin{aligned} \bar{\sigma} &= \sum_{a,b,c} \beta_{abc} \cos\left(\frac{a\pi x}{L}\right) \cos\left(\frac{b\pi y}{L}\right) \cos\left(\frac{c\pi z}{L}\right), \\ \bar{\pi}^1 &= \sum_{a,b,c} \alpha_{abc} \sin\left(\frac{a\pi x}{L}\right) \cos\left(\frac{b\pi y}{L}\right) \cos\left(\frac{c\pi z}{L}\right) \end{aligned} \quad (20)$$

and similarly for the components  $\bar{\pi}^2$  and  $\bar{\pi}^3$  which can be obtained from  $\bar{\pi}^1$  by using the transformations (15) and (17). Here we will take  $\beta_{abc} = \beta_{bca} = \beta_{cab}$ .

## IV. NUMERICAL RESULTS

In our numerical analysis, we minimize the static energy functional (11) with respect to the coefficients of the Fourier expansion (20) using the numerical optimization algorithm SNOPT [24]; the relative errors are lower than  $10^{-6}$ . A typical number of terms in the general Fourier expansion, which is necessary to obtain a solution, is about 40. To verify the results in some cases we extend it up to 100. As a consistency check we also verify numerically the results reported in Refs. [5–8] for the usual Skyrme model without potential.

First, we consider crystals in the general Skyrme model (1) with different choices of the potentials, (7), (8), and (9), and investigate the effect of the presence of the sextic term. We fix the parameters of the model as  $a = b = m_\pi = 1$  and study dependency of the normalized energy  $E/B$  of the Skyrme crystal versus the volume of the unit cell  $V/B$  for different potentials in the cases of the usual  $c = 0$  submodel and  $c = 1$  general model. In our consideration we fix  $\alpha = 1$  for the potentials (7) and (8) and take  $\alpha = 2$  for the mixed potential (9).

First, we consider in detail the dependency of the normalized energy of the crystal  $E/B$  on the volume of the unit cell. Numerical evaluation shows that in all cases these functions have a minimum at some value of the volume; see Fig. 1. The energy rapidly grows as the volume of the cell tends to zero and, as the volume increases, it slowly approaches the energy of the single isolated  $B = 1$  Skyrmion in the corresponding model. As expected, the deepest minimum of the energy corresponds to the case of the Skyrme model without the potential; the highest minimum corresponds to the model with the usual pion

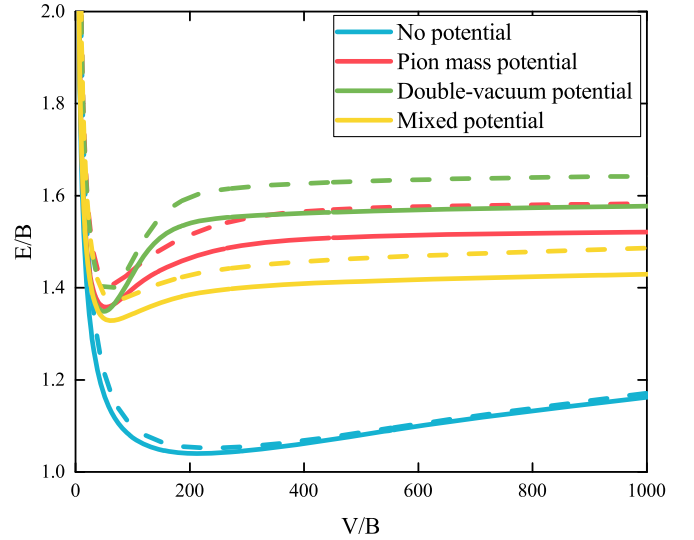


FIG. 1. Normalized energy  $E/B$  versus volume per topological charge  $V/B$  for Skyrme crystals in the general model with potentials (7), (8), and (9) for  $c = 0$  (solid lines) and  $c = 1$  (dashed lines).

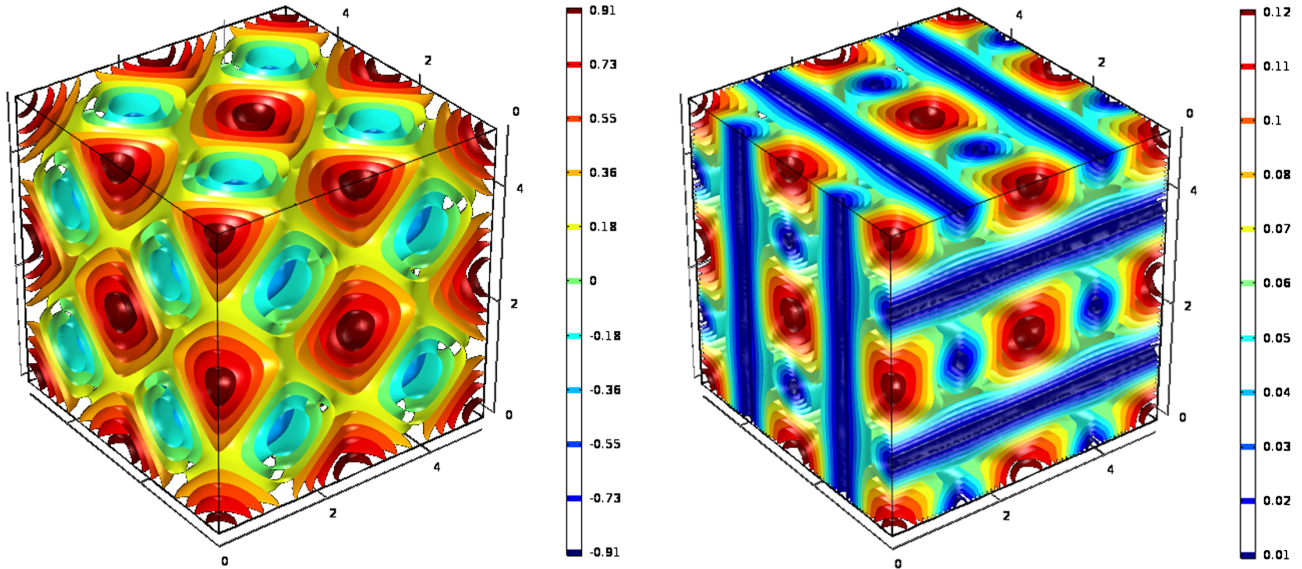


FIG. 2. Level sets of the  $\sigma$  component of the Skyrme field (left panel) and the topological charge density  $B_0$  (right panel) for the bcc Skyrmion lattice in the model (11) with  $a = 1/2$ ,  $b = 1/4$ ,  $c = 1$ ,  $m_\pi = 1$ , and the pion mass potential.

mass potential. The position of the minimum also depends on the type of the potential, we found that the lowest density minimum corresponds to the model without the potential, as seen in the Fig. 1. Evidently, the highest density minimum corresponds to the model with the double-vacuum potential (8).

Our results show that the inclusion of the sextic term always increases the energy of the crystal. Indeed, this term effectively corresponds to repulsion, it also slightly shifts the position of the minima of the energy toward lower values of density. On the other hand, inclusion of the

potential of any type yields the opposite effect: shifting the position of the corresponding minima towards higher density, the corresponding value of the minimal energy slightly increases.

As expected, we found that the structure of the solutions depends both on the type of the potentials and on the density of the configurations. Recall that there are three phases of the Skyrme crystal: the bcc lattice of half-Skyrmions with symmetries (13)–(16), which is typical for the high densities; the sc lattice of half-Skyrmions with symmetries (14), (15), (17), and (19), which exist at

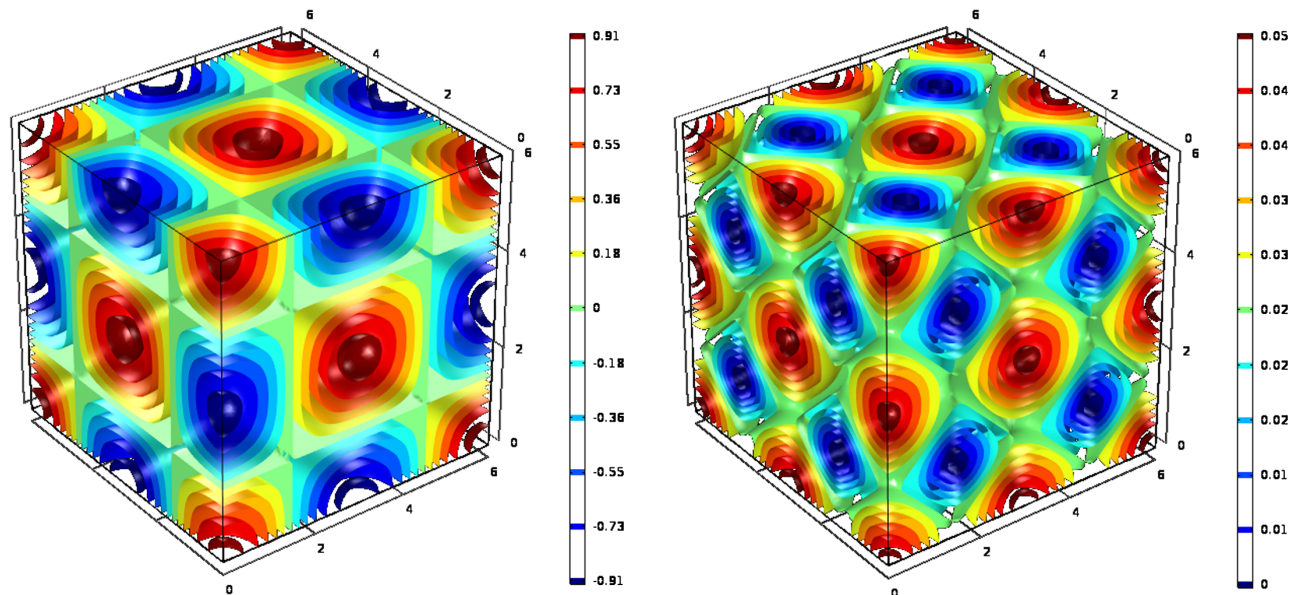


FIG. 3. Level sets of the  $\sigma$  component of the Skyrme field (left panel) and the topological charge density  $B_0$  (right panel) for the sc half-Skyrmion lattice in the model (11) with  $a = 1/2$ ,  $b = 1/4$ ,  $c = 1$ , and pion mass potential.

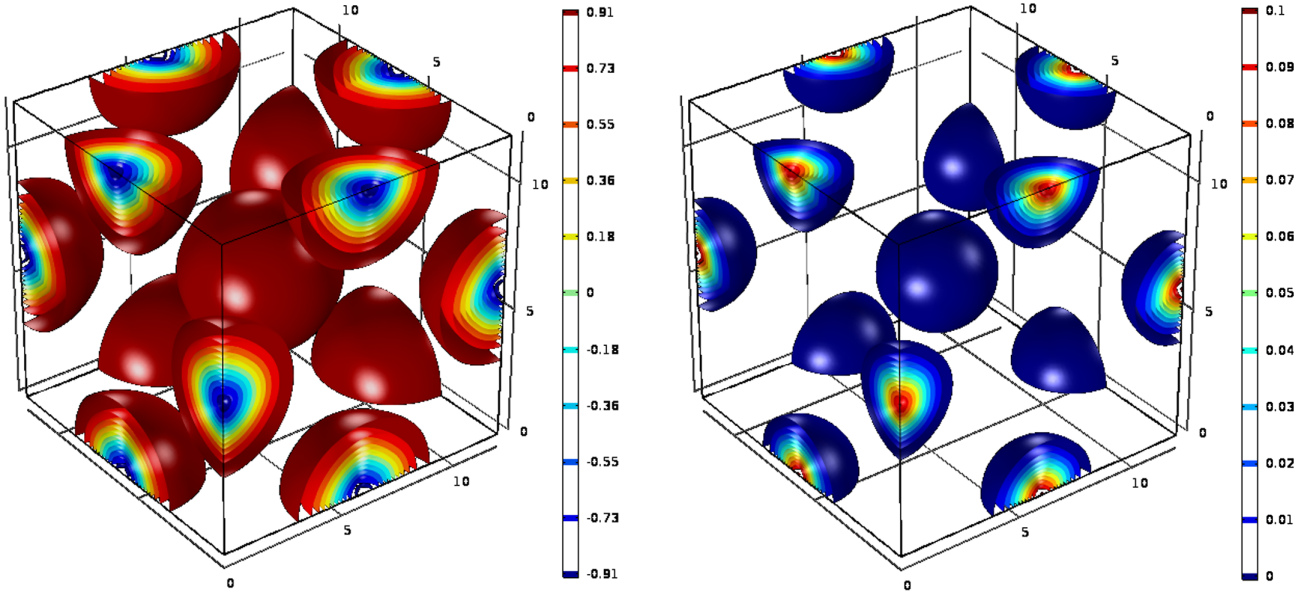


FIG. 4. Level sets of the  $\sigma$  component of the Skyrme field (left panel) and the topological charge density  $B_0$  (right panel) for the fcc Skyrmion lattice in the model (11) with  $a = 1/2$ ,  $b = 1/4$ ,  $c = 1$ ,  $m_\pi = 1$ , and the pion mass potential.

medium values of the density; and the fcc lattice of Skyrmons with symmetries (14), (15), (17), and (18), which is typical for low densities. In Figs. 2, 3, and 4 we display the typical patterns of the level sets of the  $\sigma$  component of the Skyrme field and the topological charge densities for these three types of the Skyrme crystal.

Note that in the sextic model the situation can be different; also the structure of the minimal energy configuration depends on the presence and on the particular type of the potential term. We have found that, in the absence of the potential of any type, the Skyrme crystal may exist in all three phases mentioned above. Thus, as the density of the crystal increases, two consequent phase transitions occur, one of which is of the first order and another one is of the second order. The presence of the potential term affects the phases of the Skyrme crystal in different ways depending on the explicit form of the potential.

First, we observe that the potential of any type always decreases the critical value of the volume of the unit cell, at which the transition from the sc lattice to the fcc lattice occurs. However, it almost does not affect the critical value of the density at which the second phase transitions from the fcc lattice, or at which the bcc lattice to the high-density sc phase of half-Skyrmion lattice occurs.

Second, we have found that in the case of the usual pion mass potential (7) the sc phase of the Skyrme crystal does not exist as a global minimum for any values of the density; thus, in this case in the model with or without the sextic term, there is only one phase transition between the bcc-lattice and the fcc-lattice phases.

Third, we observe that in the general model with the double-vacuum potential (8) all three phases of the Skyrme

crystal may exist. In a contrast, in the general model (1) with the mixed potential (9), all these phases exist only in the  $c = 0$  submodel without the sextic term. However, similar to the model with the usual pion mass term, there are only two phases of the Skyrme crystal in the general case  $c \neq 0$ , the bcc and the fcc lattices.

In all cases, the inclusion of the sextic term always increases the critical value of the density, at which the corresponding phase transitions occur. In Fig. 5, we represent the results of the numerical analysis of the

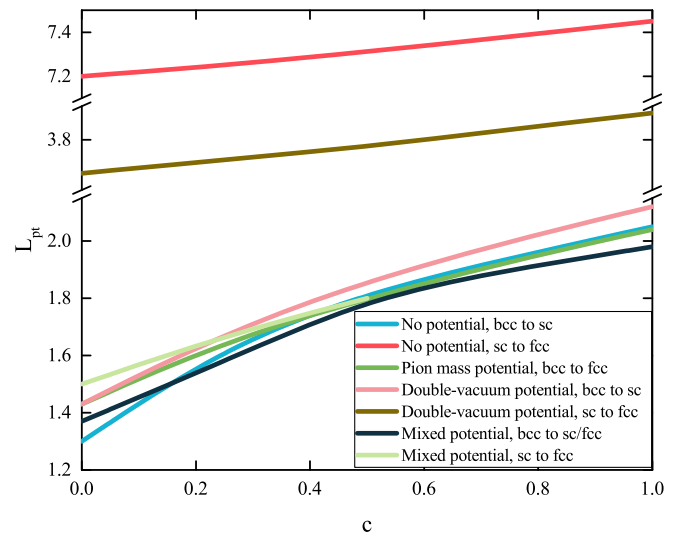


FIG. 5. Critical value of the size of the unit cell  $L_{pr}$ , at which the corresponding phase transition occurs, as functions of the coupling constant  $c$  for all phase transitions in the general Skyrme crystal at  $a = b = 1$ ,  $m_\pi = 1$ , and various choices of the potentials.

dependencies of the critical value of the size of the unit cell  $L_{pt}$ , for which the corresponding phase transition is taking place, on the increase of the coupling constant  $c$ .

### V. SKYRME CRYSTALS IN THE SUBMODELS OF THE GENERAL SKYRME MODEL

In this section we study the properties of Skyrmion crystals in various submodels of the general  $\mathcal{L}_{0246}$  model with higher-derivative terms (1). Here we make use of the abbreviated notations  $\mathcal{L}_{ijk}$  to label submodels of different types. Thus, in the previous section we discussed the usual massless Skyrme model  $\mathcal{L}_{24}$ , the Skyrme model with potential  $\mathcal{L}_{024}$ , and the submodel  $\mathcal{L}_{246}$ , which corresponds to the generalized theory (1) without potential.

It is known that the submodel  $\mathcal{L}_{06}$ , where the usual Skyrme term is replaced with a sextic term proportional to the square of the topological current, supports self-dual solutions [11,20]. Further, the structure of the solutions strongly depends on the explicit form of the potential [13,22]. In particular, for the generalized pion mass potential (7) with  $\alpha < 3$ , the self-dual solutions are compactons with nonanalytic behavior on the boundary of the support. Analogously, the submodel  $\mathcal{L}_{046}$  with the usual pion mass potential also supports compacton solutions.

For the sake of simplicity we further restrict our consideration to the family of models with the usual pion mass potential:

$$\mathcal{V} = \text{Tr} \left( \frac{\mathbb{1} - U}{2} \right). \quad (21)$$

With this particular choice of the potential (21), the solutions of the self-dual  $\mathcal{L}_{06}$  submodel are spherically symmetric compactons [11,20]:

$$\sigma = \begin{cases} r^2 \left( \frac{m_\pi^2}{2|B|\sqrt{c}} \right)^{\frac{1}{3}} - 1 & r \in [0, r_{cr} = \sqrt{2} \left( \frac{2|B|\sqrt{c}}{m_\pi^2} \right)^{\frac{1}{3}}], \\ 0 & r \geq r_{cr} \end{cases} \quad (22)$$

with the energy

$$E = \frac{128\pi\sqrt{2}cm_\pi^2}{15} |B|. \quad (23)$$

Thus, the solitons of the  $\mathcal{L}_{06}$  submodel at zero temperature behave like an incompressible system of noninteracting liquid droplets. Further, there is no crystal of any type in this submodel. Indeed, the size of the compacton  $r_{cr} \sim |B|^{\frac{1}{3}}$ . Therefore, the energy density distribution does not depend on the distribution of the topological charge in the droplets. The total topological charge of the system of noninteracting compactons is equally distributed among the available volume; as the size of the cell is decreasing, the droplets

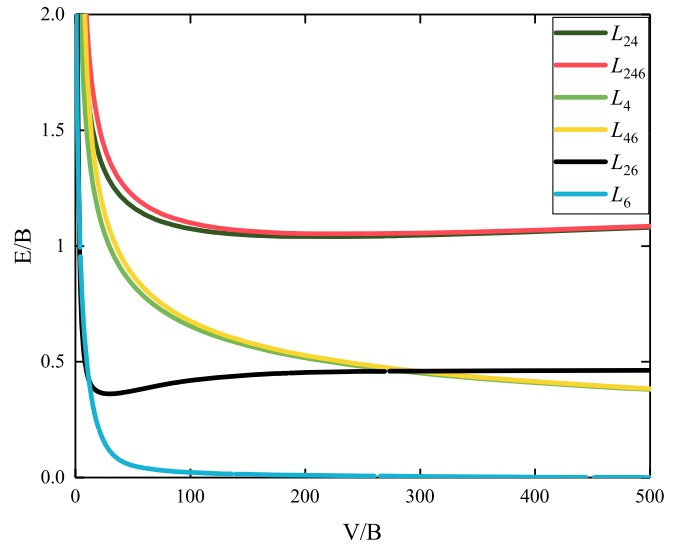


FIG. 6. Normalized energy  $E/B$  versus volume per topological charge  $V/B$  for Skyrme crystals in the general model with pion mass potential (21) and for various submodels.

merge to decrease the energy. Finally, they form a single incompressible sphere with radius  $\sqrt{2} \left( \frac{2|B|\sqrt{c}}{m_\pi^2} \right)^{\frac{1}{3}}$  within which all the topological charge  $|B|$  is concentrated.

The Skyrme crystals in the submodels  $\mathcal{L}_{26}$ ,  $\mathcal{L}_{4}$ , and  $\mathcal{L}_{46}$  can be considered without the potential term since its effect is not very significant in these cases. In Fig. 6 we display dependencies of the normalized energy  $E/B$  on the volume of the unit cell for these crystals (cf Fig. 1). Numerical evaluation shows that for the submodel  $\mathcal{L}_{26}$  without the Skyrme term, this dependency is qualitatively the same. As in the general model, the energy per cell infinitely increases as the cell volume is decreasing to zero and it tends to the energy of the single unit charge soliton as the volume increases. The value of the minimum of the energy is, however, lower than in the full model. It corresponds to the higher value of density; see Fig. 6. Indeed, it was shown by Adam and Wereszczynski [25] that for the  $\mathcal{L}_{26}$  submodel the new energy bound is

$$E \geq \frac{a}{3c} |B| \quad (24)$$

where  $E$  is the normalized energy per unit cell. In our case we set  $a = c = 1$ , thus it yields the bound  $\frac{E}{B} \geq \frac{1}{3}$ , while our numerical simulations give the value of the minimal energy  $E_{\min} \sim 0.355|B|$  at the lattice size  $L_0 = 2.37$ . Thus, the minimum of the energy is just 1.5% above the corresponding energy bound for the  $\mathcal{L}_{26}$  submodel [25].

Similar to the case of the usual Skyrme model, the minimal energy configuration corresponds to the same sc lattice of half-Skyrmions. Further, the phase structure of the Skyrme crystal in this submodel also possesses the phases we observed in the full model; thus, we may conclude that the minimal energy crystals in the  $\mathcal{L}_{26}$  and  $\mathcal{L}_{246}$  submodels are quite similar for all range of values of the density.

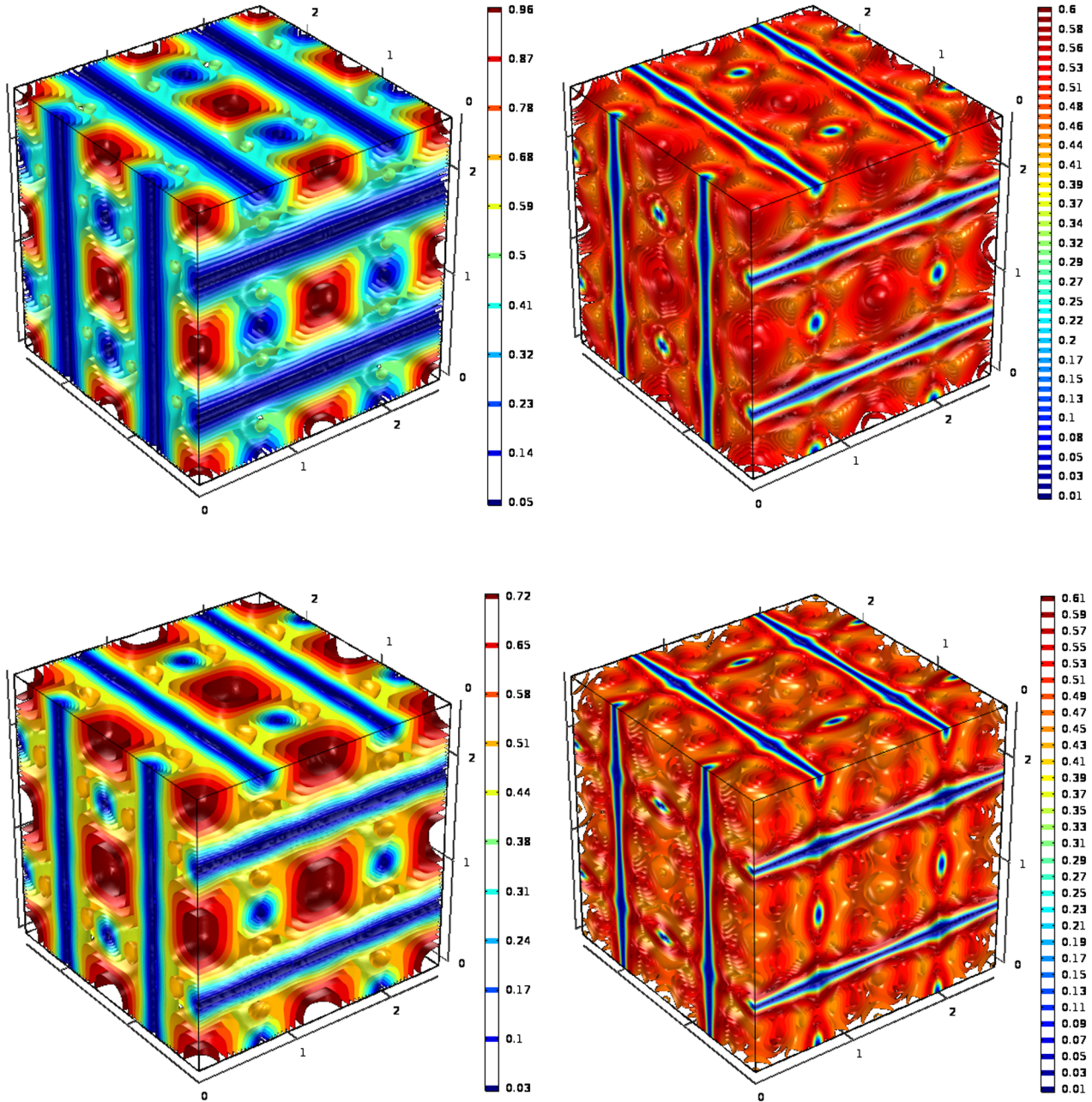


FIG. 7. Level sets of the topological charge density  $B_0$  for the Skyrme crystal in the pure  $\mathcal{L}_4$  submodel (left upper panel), in the  $\mathcal{L}_{26}$  submodel (right upper panel), in the  $\mathcal{L}_{46}$  submodel (left lower panel), and in the pure  $\mathcal{L}_6$  submodel (right lower panel) at  $L = 1$ .

The pattern we observed in the case of  $\mathcal{L}_{46}$  submodel is quite different from what we discussed above. First, the dependency of the normalized energy on the volume of the unit cell does not possess a minimum. It monotonically decreases from infinity, in the limit of zero volume, to zero, as  $L \rightarrow \infty$ ; see Fig. 6. Indeed, there is no usual kinetic term in such a model; a stable soliton solution cannot exist on  $\mathbb{R}^3$ . However, imposing the boundary condition of triple periodicity in a crystal effectively sets the theory on a torus  $T^3$ . It also provides a natural scale parameter of the model, the lattice period  $L$ ; hence, the

solitons may be bounded in the Skyrme crystal. Further, it is even possible to truncate the model to the pure Skyrme  $\mathcal{L}_4$  or even  $\mathcal{L}_6$  crystals. Our numerical computations show that the normalized energy of the  $\mathcal{L}_4$  crystal qualitatively depends on the volume of the unit cell in the same way, as in the  $\mathcal{L}_{46}$  submodel; see Fig. 6.

The second feature of the Skyrme crystals in  $\mathcal{L}_4$  and  $\mathcal{L}_{46}$  submodels above is that there we do not observe the fcc-lattice phase. Thus, there is only one phase transition from the bcc lattice to the sc lattice of half-Skyrmions. As in the case of the full model, the presence of the sextic term yields



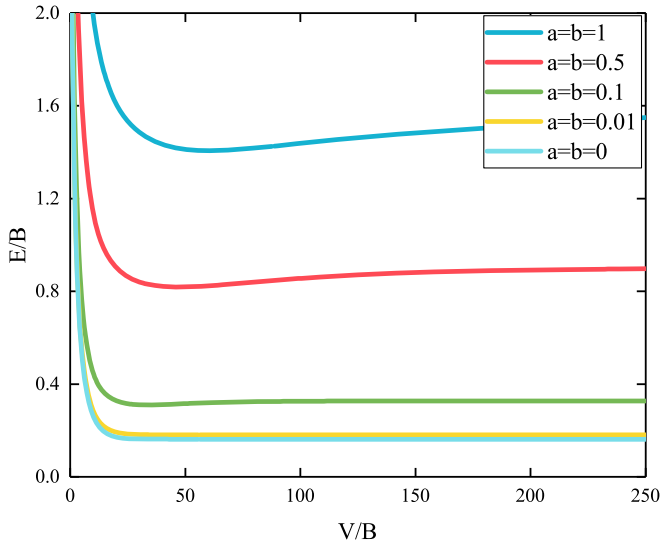


FIG. 8. Normalized energy  $E/B$  versus volume per topological charge  $V/B$  for Skyrme crystals in the near-BPS model for a set of different decreasing values of  $a = b$ .

some minor increase of the energy of the crystal, as well as the values of the volume of the cell, at which the normalized energy has a minimum, or the phase transition occurs.

The peculiarity of the  $\mathcal{L}_6$  crystal is that the corresponding term is strongly repulsive; the value of the density should be rather high to stabilize the configuration. Numerical simulations indicate that this crystal may exist only in the bcc phase. Similar to the limiting behavior of the Skyrme crystal in the  $\mathcal{L}_{26}$  submodel, in the limit of zero volume the normalized energy of the  $\mathcal{L}_6$  crystal diverges, as it is seen in Fig. 6.

For comparison we display the distribution of the topological charge density in the  $\mathcal{L}_4$ ,  $\mathcal{L}_{26}$ ,  $\mathcal{L}_{46}$ , and  $\mathcal{L}_6$  submodels at the same value of the lattice size  $L = 1$  in Fig. 7. In all cases, the Skyrme crystal is in the bcc phase, so the patterns we observe are similar.

### A. Skyrme crystals in near-self-dual model

Let us now discuss how the structure and properties of the Skyrme crystal change as the full model approaches the self-duality limit. We consider the model (1) with the pion mass potential (21) fixing the parameters  $c = m_\pi = 1$  and gradually decrease the other two coupling constants. It is convenient for our purposes to set  $a = b = \lambda$ ,  $\lambda \in [0, 1]$ .

Our numerical simulations show that, as expected, the decreasing of these parameters yields a significant decrease of the value of the energy per unit cell; see Fig. 8. We observe that the minimal energy of the configuration decreases almost linearly from the value  $E_{\min} = 1.396$  at  $\lambda = 1$  to the minimal value  $E_{\min} = 0.161$  at  $\lambda = 0$ .

The second observation is that the critical value of the lattice spacing, at which the phase transition from the bcc lattice of half-Skyrmions to the fcc lattice of Skyrmions occurs, swiftly increases, as the system approaches the self-duality limit. Also at the critical value of parameter  $\lambda \approx 0.4$ , the new third phase appears. In this phase the Skyrme crystal is transformed into the Klebanov's sc lattice. Recall that the generators of symmetry of this phase are (13)–(15) and the transition between the Klebanov's sc low-density phase of single Skyrmions and the bcc high-density phase of the Skyrme crystal is of second order. In Fig. 9, which supplements Figs. 2–4, we display the spatial distribution of the  $\sigma$  component of the Skyrme field and the topological charge density of the Skyrme field and the topological

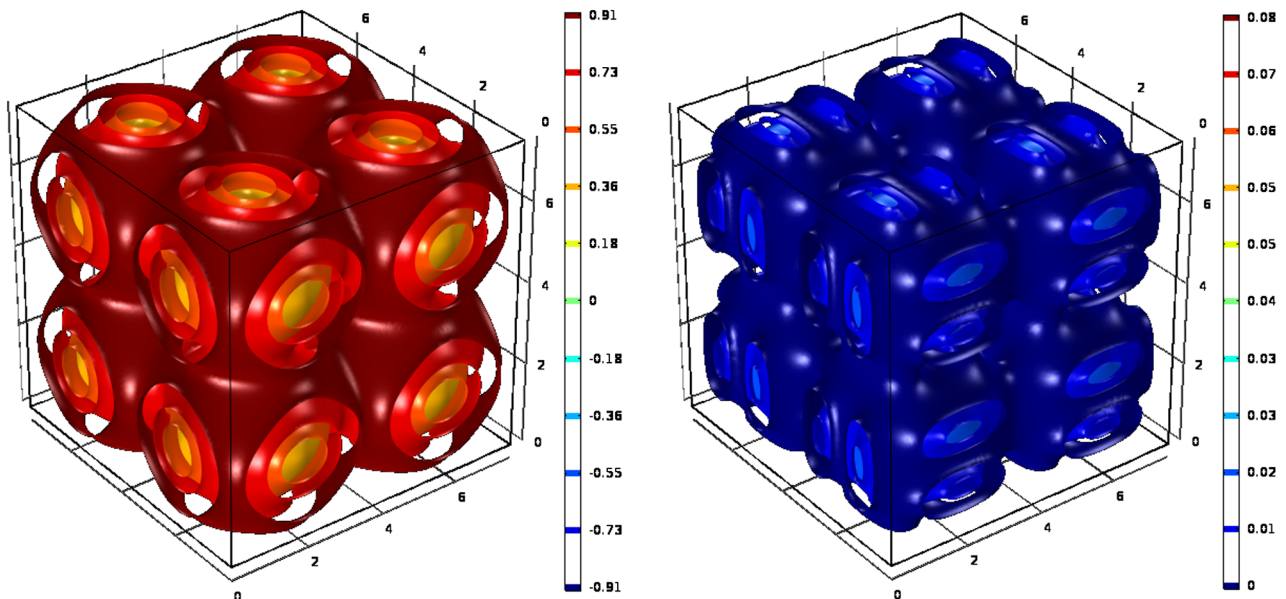


FIG. 9. Level sets of the  $\sigma$  component of the Skyrme field (left panel) and the topological charge density  $B_0$  (right panel) for the Skyrme crystal lattice in the general  $\mathcal{L}_{0246}$  model with  $a = b = 0.1$ ,  $c = 1$ ,  $m_\pi = 1$ , and the pion mass potential.

charge density  $B_0$  for such a simple cubic lattice of Skyrmions at  $\lambda = 0.1$ .

Further, as the value of the parameter  $\lambda$  continues to decrease, the contributions to the total energy functional (11), which come from the  $\mathcal{L}_2 + \mathcal{L}_4$  terms and from the  $\mathcal{L}_0 + \mathcal{L}_6$  terms, become of the same order. Then the phase transition from the sc lattice of Skyrmions to the fcc lattice is no longer observed and only two phases of the Skyrme crystal remain. The fcc-lattice phase disappears at  $\lambda \approx 0.3$ . With the further decrease of  $\lambda$ , the point of transition from the bcc lattice to the simple sc lattice of Skyrmions shifts towards lower values of the density, approaching the limiting value  $8r_{cr}^3$ . At this point  $r_{cr}$  is just the radius of the compacton (22). At the same time, the normalized energy per cell approaches the value of the energy of a single compacton (23). Considering the near-BPS submodel, we found that there are indications of the phase transition from a low-density quasi-liquid phase to the high-density symmetric phase of the Skyrmionic matter. Finally, the solitons become localized on a compact support and the system does not represent a crystal anymore. Instead it can be treated as an incompressible fluid on the torus  $T^3$ .

## VI. CONCLUSIONS

We have investigated the properties of the Skyrme crystals in the general Skyrme model with the higher-derivative sextic term being the topological current squared. This model possesses various limiting cases, among which are the usual Skyrme model with or without the pion mass term and the self-dual  $\mathcal{L}_{06}$  submodel. Investigating the pattern of phase transition in these crystalline systems we found that, depending on the density of the configuration, the general Skyrme crystal with minimal energy may exist in four different phases, which correspond to the low-density sc lattice of Skyrmions (Klebanov's crystal), bcc lattice of half-Skyrmions, the fcc lattice of Skyrmions, and the high-density phase of the sc lattice of half-Skyrmions. The phase transition between the phases of the fcc lattice of Skyrmions and the sc lattice of half-Skyrmions is of the second order. Also the transition between the Klebanov's phase of the sc lattice of single Skyrmions and the bcc lattice is of second order whereas the transition from the phase of the fcc lattice of Skyrmions to the bcc lattice half-Skyrmions is of first order.

We found that the addition of the repulsive sextic term to the usual Skyrme model always increases the energy of the

crystal shifting the minima of the total energy toward lower values of density. In the presence of the potential term, the generalized minimal energy Skyrme crystal may exist in four phases mentioned above; the Klebanov's phase appears in the model with the pion mass potential as the contributions of the  $\mathcal{L}_2$  and the  $\mathcal{L}_4$  terms becomes less significant than the energy of the strongly repulsive term  $\mathcal{L}_6$  and the potential  $\mathcal{L}_0$ . Further, the structure of the Skyrme crystal depends also on the type of the potential of the model, which, depending on the values of the parameters of the model, may eliminate some of these phase transitions.

We also considered crystalline structures in the submodels of the general Skyrme model. The most interesting finding is that the Skyrme crystal may exist in the pure  $\mathcal{L}_4$  and  $\mathcal{L}_6$  models. The pattern of the phase transitions in the first of these submodels, as well as in the similar  $\mathcal{L}_{46}$  submodel, is restricted to just one transition from the bcc lattice to the high-density phase of the sc lattice of half-Skyrmions and the normalized energy monotonically decreases as the lattice spacing increases. We also verified that the energy of the Skyrme crystals in the  $\mathcal{L}_{26}$  submodel attains an absolute minimum at some critical value of the lattice spacing. This minimum is just 1.5% above the corresponding energy bound for this submodel [25,26].

Considering the near-BPS submodel, we found that there are indications of the phase transition from a low-density quasi-liquid phase to the high-density symmetric phase of the Skyrmionic matter.

As a direction for future work, it would be interesting to study the generalized Skyrme crystals at finite temperature; the pattern of phase transitions in this case can be very different. It might be also interesting to consider generalized Skyrme lattices with hexagonal symmetry, considered by Battye and Sutcliffe in the usual Skyrme model [27].

## ACKNOWLEDGMENTS

We would like to thank A. Wereszczynski and C. Adam for relevant discussions and suggestions. Y. S. gratefully acknowledges support from the Russian Foundation for Basic Research (Grant No. 16-52-12012), the Ministry of Education and Science of Russian Federation, Project No. 3.1386.2017, and Deutsche Forschungsgemeinschaft (Grant No. LE 838/12-2). He would like to thank H. Nicolai and the staff of the AEI Golm for hospitality and support during the completion of this work.

---

[1] T. H. R. Skyrme, A non-linear field theory, *Proc. R. Soc. A* **260**, 127 (1961); A unified field theory of mesons and baryons, *Nucl. Phys.* **31**, 556 (1962).

[2] E. Braaten, S. Townsend, and L. Carson, Novel structure of static multisoliton solutions in the Skyrme model, *Phys. Lett. B* **235**, 147 (1990).

- [3] R. A. Battye and P. M. Sutcliffe, Symmetric Skyrmions, *Phys. Rev. Lett.* **79**, 363 (1997).
- [4] C. J. Houghton, N. S. Manton, and P. M. Sutcliffe, Rational maps, Monopoles and Skyrmions, *Nucl. Phys.* **B510**, 507 (1998).
- [5] I. R. Klebanov, Nuclear matter in the skyrme model, *Nucl. Phys.* **B262**, 133 (1985).
- [6] A. S. Goldhaber and N. S. Manton, Maximal symmetry of the Skyrme crystal, *Phys. Lett. B* **198**, 231 (1987).
- [7] L. Castillejo, P. S. J. Jones, A. D. Jackson, J. J. M. Verbaarschot, and A. Jackson, Dense Skyrmion systems, *Nucl. Phys.* **A501**, 801 (1989).
- [8] M. Kugler and S. Shtrikman, A new Skyrmion crystal, *Phys. Lett. B* **208**, 491 (1988).
- [9] N. Manton and P. Sutcliffe, *Topological Solitons* (Cambridge University Press, Cambridge, 2004).
- [10] R. Battye and P. Sutcliffe, Skyrmions with massive pions, *Phys. Rev. C* **73**, 055205 (2006).
- [11] C. Adam, J. Sanchez-Guillen, and A. Wereszczynski, Skyrme-Type Proposal for Baryonic Matter, *Phys. Lett. B* **691**, 105 (2010).
- [12] P. Sutcliffe, Skyrmions in a truncated BPS theory, *J. High Energy Phys.* **04** (2011) 045.
- [13] M. Gillard, D. Harland, and M. Speight, Skyrmions with low binding energies, *Nucl. Phys.* **B895**, 272 (2015).
- [14] S. B. Gudnason, Loosening up the Skyrme model, *Phys. Rev. D* **93**, 065048 (2016).
- [15] L. Marleau, All orders skyrmions, *Phys. Rev. D* **45**, 1776 (1992).
- [16] J. A. Neto, A note in the Skyrme model with higher derivative terms, *J. Phys. G* **20**, 1527 (1994).
- [17] I. Floratos and B. Piette, Multiskyrmion solutions for the sixth order Skyrme model, *Phys. Rev. D* **64**, 045009 (2001).
- [18] D. Harland, Topological energy bounds for the Skyrme and Faddeev models with massive pions, *Phys. Lett. B* **728**, 518 (2014).
- [19] By analogy with the corresponding monopole solutions of the Yang-Mills-Higgs model, which satisfy the BPS equations, the self-dual solutions of the integrable Skyrme submodel are usually referred to as “BPS Skyrmions.” This of course is an abuse of terminology.
- [20] C. Adam, J. Sanchez-Guillen, and A. Wereszczynski, BPS Skyrme model and baryons at large  $N_c$ , *Phys. Rev. D* **82**, 085015 (2010).
- [21] Note that for some particular choices of  $\mathcal{V}$ , the linearized excitations are massless; therefore,  $m_\pi$  is not always associated with the pion mass.
- [22] C. Adam, C. D. Fosco, J. M. Queiruga, J. Sanchez-Guillen, and A. Wereszczynski, Symmetries and exact solutions of the BPS Skyrme model, *J. Phys. A* **46**, 135401 (2013).
- [23] T. Weidig, The baby Skyrme models and their multi-Skyrmions, *Nonlinearity* **12**, 1489 (1999).
- [24] P. Gill, W. Murray, and M. A. Saunders, SNOPT: An SQP algorithm for large-scale constrained optimization, *SIAM Rev.* **47**, 99 (2005).
- [25] C. Adam and A. Wereszczynski, Topological energy bounds in generalized Skyrme models, *Phys. Rev. D* **89**, 065010 (2014).
- [26] C. Adam, M. Haberichter, and A. Wereszczynski, Skyrme models and nuclear matter equation of state, *Phys. Rev. C* **92**, 055807 (2015).
- [27] R. A. Battye and P. M. Sutcliffe, A Skyrme lattice with hexagonal symmetry, *Phys. Lett. B* **416**, 385 (1998).